Acta Crystallographica Section B
Structural Science
ISSN 0108-7681

X-ray diffraction study for one-dimensional ionic conductors $K_x(Ga_{1-y}Al_y)_{2+x}Ti_{2-x}O_7$ ($x \simeq 0.14$, $y \simeq 0.10, 0.23, 0.39$)

Yuichi Michiue[a]* and Shinzo Yoshikado[b]

[a]Advanced Materials Laboratory, National Institute for Materials Science, 1-1 Namiki, Tsukuba, Ibaraki 305-0044, Japan, and [b]Department of Electronics, Doshisha University, Kyotanabe 610-0321, Japan

Correspondence e-mail: michiue.yuichi@nims.go.jp

Received 17 March 2005
Accepted 29 September 2005

The structures of one-dimensional ionic conductors $K_x(Ga_{1-y}Al_y)_{2+x}Ti_{2-x}O_7$ ($x \simeq 0.14$, $y \simeq 0.10, 0.23, 0.39$) were refined by single-crystal X-ray diffraction. A one-dimensional tunnel-like space with a large cross section is formed by the linkage of coordination polyhedra of the metal and oxygen ions; K ions are distributed in the tunnel. Significant differences were seen in structures with different Al content; these differences could be explained by considerations in crystal chemistry. The probability density functions (PDFs) of the K ion were obtained using up to fourth-order terms of the atomic displacement parameters. The joint PDFs for the K ion have clarified that a K conduction path deviates slightly from the central axis of the tunnel in all the samples. In contrast with the usual one-dimensional ionic conductors, no distinct *bottleneck effect* was observed from the joint-PDFs and one-particle potentials.

1. Introduction

One-dimensional ionic conductors show high anisotropy in their ionic conductivity. In general, materials have structures with a one-dimensional tunnel of a large cross section; the mobile ions are accommodated in the tunnel. The ionic conduction of $A_xGa_{2+x}Ti_{2-x}O_7$ (A = K, Rb, Cs) with an octagonal one-dimensional tunnel has been studied by AC impedance measurements (Yoshikado *et al.*, 1988, 1990, 1996, 1999), NMR (Onoda *et al.*, 1989, 1990) and X-ray diffraction studies (Watanabe *et al.*, 1988, 1990, 1992). The host structure of $K_xGa_{2+x}Ti_{2-x}O_7$ ($x \simeq 0.14$; Fig. 1*a*) is constructed by the linkage of coordination polyhedra of metal (Ga, Ti) and oxygen ions (Watanabe, Sasaki, *et. al.*, 1987). The K ions in the tunnel are mobile along **c**. In the usual one-dimensional ionic conductors the effective size of the tunnel section is smaller than that of the mobile ion. For example, the tunnel walls in hollandite one-dimensional ionic conductors are constructed by the stacking of oxygen squares. The effective size of the square is smaller than the diameter of the K ion. Therefore, it is assumed that a high energy is necessary for the K ion to go through the square, and this square of oxygen ions plays the role of the so-called *bottleneck* for the K-ion transport. On the other hand, the effective size of the tunnel section is always larger than the size of the K ion in $K_xGa_{2+x}Ti_{2-x}O_7$. The tunnel wall is composed of alternate stackings of the two squares of oxygen ions. One square consists of four O6 ions (Fig. 1*b*) and the other of the four O7 ions (Fig. 1*c*). The diagonal distances of the squares are 6.156 (11) Å for O6—O6 and 6.517 (11) Å for O7—O7. The effective diameter of the square, given by twice subtracting the ionic radius of the O ion (1.40 Å), is

3.356 Å for the O6 square and 3.717 Å for the O7 square. The values are larger than the diameter of the K ion, which is 2.74 Å [*i.e.* twice the ionic radius for the four-coordinate K (1.37 Å); Shannon, 1976]. Even though the K ion is considered to be 12-coordinate, including an additional eight oxygen ions of the second nearest group, the ionic radius of the K ion is 1.64 Å (Shannon, 1976) and the diameter is 3.28 Å. Thus, it is expected that the tunnel in $K_xGa_{2+x}Ti_{2-x}O_7$ has no *bottle-neck effect* on the K-ion conduction. This unique structural character of $K_xGa_{2+x}Ti_{2-x}O_7$ is reflected in the high ionic conductivity along the tunnel direction at microwave frequencies (Yoshikado *et al.*, 1988).

It has been reported that the Ga ion in $K_xGa_{2+x}Ti_{2-x}O_7$ is partially replaced by Al (Yoshikado *et al.*, 1992). However, the structural details of Al-substituted compounds have never been reported. In this study the structures of $K_x(Ga_{1-y}Al_y)_{2+x}Ti_{2-x}O_7$ ($x \simeq 0.14$, $y \simeq 0.10$, 0.23, 0.39) were refined by the single-crystal X-ray diffraction technique. In order to clarify the K-ion distribution in the tunnel, the probability density functions (PDFs) were obtained by applying anharmonic atomic displacement parameters (ADPs) based on the Gram–Charlier expansion (Johnson & Levy, 1974; Kuhs, 1992).

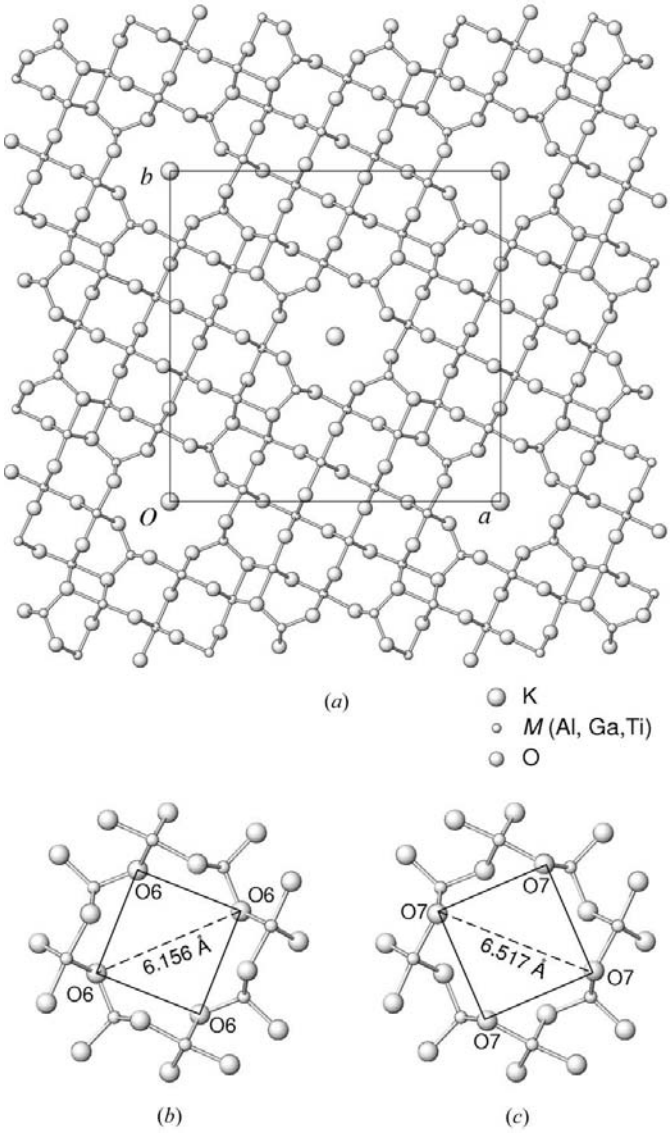

Figure 1
Structure of $K_xGa_{2+x}Ti_{2-x}O_7$ projected along **c**.

2. Experimental

Single crystals were obtained by the slow cooling method. A mixture of K_2CO_3, Ga_2O_3, Al_2O_3 and TiO_2 (K_2CO_3:Ga_2O_3:Al_2O_3:TiO_2 = 1:1-α:α:1 in a molar ratio, α = 0.1, 0.3, 0.5) was heated with K_2CO_3–MoO_3 flux (K_2CO_3:MoO_3 = 4:6 in a molar ratio) at 1573 K for 10 h. The sample was cooled to 1273 K at a rate of 4 K h^{-1} and then taken out of the furnace. The flux was dissolved in hot water to separate the crystals. As the chemical composition of the crystals obtained generally deviates from that in the flux melts, the metal contents of the crystals were estimated from electronprobe microanalyses (EPMA). The results for various α [= Al_2O_3/(Al_2O_3 + Ga_2O_3) in the flux melt] values are given in Table 1, where the data for α = 0 (*i.e.* no Al_2O_3 in the flux melt) were taken from the literature (Watanabe *et al.*, 1992). TiO_2 and K_2O contents were almost independent of α, while significant changes were observed in Ga_2O_3 and Al_2O_3 contents according to the change in α. The Al/(Al + Ga) ratio in the crystal grown, which corresponds to the y parameter in the chemical formula $K_x(Ga_{1-y}Al_y)_{2+x}Ti_{2-x}O_7$, was very similar to that in the flux melt (*i.e.* α) for α = 0.1. The deviation of y from α becomes prominent according to the increase in α. The Al/(Al + Ga) ratio in the crystal from the α = 0.5 flux melt was actually 0.39, as shown in Table 1. The crystals from the α = 0.1, 0.3 and 0.5 flux melts are, hereafter, referred to as samples (I), (II) and (III), respectively. The chemical compositions are $K_x(Ga_{1-y}Al_y)_{2+x}Ti_{2-x}O_7$ with $x \simeq 0.14$ and $y \simeq 0.10$ for sample (I), $y \simeq 0.23$ for sample (II) and $y \simeq 0.39$ for sample (III).

Details of the conditions and parameters for the X-ray diffraction data collection and refinement are given in Table 2. Four nonequivalent positions, *M*1–*M*4, were taken for the metal ions constructing the framework structure. The *M*1 position represents the tetrahedral coordination site, but *M*2–*M*4 are octahedral sites. The occupation factors in $K_xGa_{2+x}Ti_{2-x}O_7$ ($x \simeq 0.14$) were 1.0 (*M*1 site), 0.83 (*M*2), 0.31 (*M*3), 0 (*M*4) for Ga, and 0 (*M*1), 0.17 (*M*2), 0.69 (*M*3), 1 (*M*4) for Ti (Watanabe, Sasaki *et al.*, 1987). As the Al ions are expected to substitute some of the Ga ions, it was assumed that the *M*1 site is occupied by Al and Ga ions, and the *M*2 and *M*3 sites are occupied by Al, Ga and Ti ions. The *M*4 site was assumed to be fully occupied by the Ti ion during the initial stages, but significant improvements in refinement were obtained by replacing a small number of Ti ions by Ga. In addition, it is known that a small number of Ga ions were moved from the *M*1 site to an interstitial site in $K_xGa_{2+x}Ti_{2-x}O_7$ (Watanabe *et al.*, 1992). In the present crystals, the *M*5 interstitial site is allocated for these Ga ions. The occupation factors at each octahedral site (*M*2, *M*3, *M*4) were refined imposing the

Table 1
Molar contents in the crystal estimated by the electronprobe microanalysis.

α is the molar ratio $Al_2O_3/(Al_2O_3 + Ga_2O_3)$ in the flux melt. y is the Al/(Al + Ga) ratio in the crystal or the parameter in the chemical formula $K_x(Ga_{1-y}Al_y)_{2+x}Ti_{2-x}O_7$.

	α	K_2O	Ga_2O_3	Al_2O_3	TiO_2	y
$K_xGa_{2+x}Ti_{2-x}O_7$†	0	0.027	0.358	0	0.615	0
Sample (I)	0.10	0.028	0.321	0.035	0.616	0.10
Sample (II)	0.30	0.027	0.279	0.082	0.616	0.23
Sample (III)	0.50	0.026	0.214	0.139	0.621	0.39

† Data from the literature (Watanabe *et al.*, 1992).

constraint condition that the sum of the occupation factors of the metal ions (Al, Ga, Ti) is unity, while the sum of the occupation factors for metals at the *M*1 and *M*5 sites were set to unity; Occ[Al(*M*1)] + Occ[Ga(*M*1)] + Occ[Ga(*M*5)] = 1. Additional constraint conditions were imposed on occupation factors of Al and Ga, so that the metal contents from the refinement are equal to those from EPMA. Namely, Occ[Al(*M*1)] + Occ[Al(*M*2)] + Occ[Al(*M*3)] was set to 0.21 [sample (I)], 0.49 [sample (II)] and 0.84 [sample (III)], and Occ[Ga(*M*1)] + Occ[Ga(*M*2)] + Occ[Ga(*M*3)] + Occ[Ga(*M*4)] + Occ[Ga(*M*5)] was 1.93 [sample (I)], 1.65 [sample (II)] and 1.30 [sample (III)]. It was also assumed that the number of Ti ions in each sample was equal to that in $K_xGa_{2+x}Ti_{2-x}O_7$ ($x \simeq 0.14$), *i.e.* Occ[Ti(*M*2)] + Occ[Ti(*M*3)] + Occ[Ti (*M*4)] = 1.86, which is supported by the result from EPMA.

Third- and fourth-order Gram–Charlier terms (Johnson & Levy, 1974; Kuhs, 1992) were introduced for the atomic displacement parameters of the K atom, which gave realistic PDFs with no significant negative regions. The maximum and minimum residual peaks in the tunnel (the volume with $-0.05 \le x \le 0.05$, $-0.05 \le y \le 0.05$ and $0 \le z \le 1$ was considered for convenience) for harmonic ADP models, 1.44 and −1.11 e Å^{-3} in sample (I), 1.13 and −1.18 e Å^{-3} in sample (II), and 2.23 and −1.31 e Å^{-3} in sample (III), were changed to 1.23 and −1.18 e Å^{-3} in sample (I), 1.11 and −1.17 e Å^{-3} in sample (II), 2.28 and −1.31 e Å^{-3} in sample (III) for the anharmonic ADP models. Difference Fourier maps at $z = \zeta$ ($|\zeta| \le ca$ 0.2) for sample (I) with the harmonic model revealed four positive peaks at positions displaced from the center, as shown in Fig. 2(*a*) for $\zeta = 0$. The residual densities were negative at the center (0, 0, ζ) of the maps. These facts indicate that the K conduction path splits into four branches deviating from the central axis of the tunnel, which is probable from a crystal chemistry viewpoint, as discussed in the following section. Refinements with split-atom models with the K site away from the tunnel axis were unsuccessful because of the strong correlations between parameters. On the other hand, the anharmonic model was a good approximation of the complicated K-ion distribution mentioned above, giving a map with lower residuals than those in the harmonic model at the $z = 0$ section (Fig. 2*b*). Thus, the anharmonic model describes the structure of sample (I) better than the harmonic model. However, the splitting of the conduction path is rather ambiguous for samples (II) and (III) from the residual density maps (given as supplementary material).[1] It is difficult to judge the validity of models by comparing the residual maps of specific sections, because the K distributions in the present samples are almost continuous along the tunnel. In order to confirm the validity of the introduction of anharmonic ADPs, Hamilton's method (Hamilton, 1965) was used to check the following hypothesis: 'The K ion is described adequately by the harmonic ADP model'. As the number of parameters is 79 for harmonic models and 86 for anharmonic models, the dimension of the hypothesis is 7 (= 86 − 79). The numbers of degrees of freedom for the refinement are 2731 (= 2817 − 86) for sample (I), 2725 (= 2811–86) for sample (II) and 2623 (= 2709–86) for sample (III). Thus, the critical values for the 0.5% significance level are $R_{7,2731,0.005}$ = 1.0038 for sample (I),

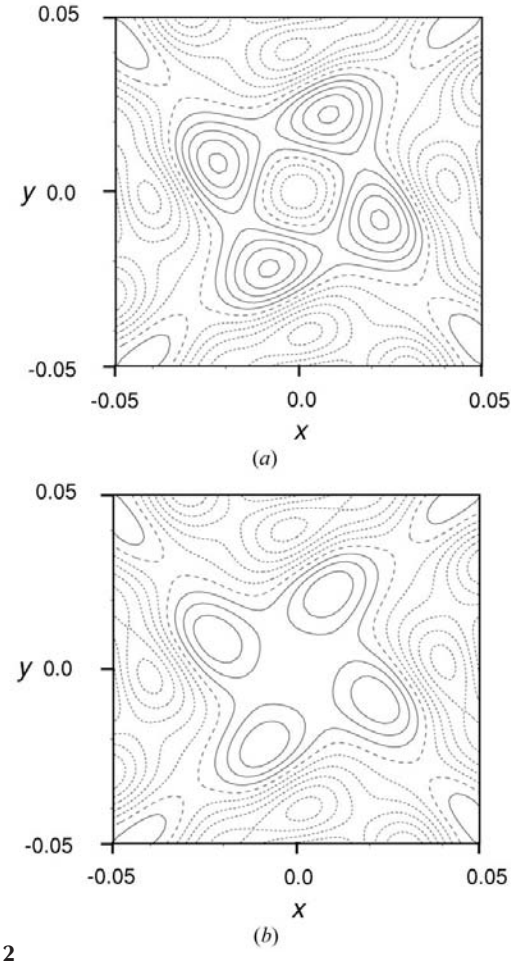

Figure 2
Difference Fourier maps at the $z = 0$ section for sample (I) from (*a*) the harmonic model and (*b*) the anharmonic model. Contour intervals are 0.2 e Å^{-3}. The solid and dotted lines represent positive and negative densities, respectively; the broken lines are zero levels.

[1] Supplementary data for this paper are available from the IUCr electronic archives (Reference: LC5028). Services for accessing these data are described at the back of the journal.

Table 2
Crystallographic data and conditions for data collection and refinement.

	Sample (I)	Sample (II)	Sample (III)
Crystal data			
Chemical formula	$Al_{0.21}Ga_{1.93}K_{0.152}O_7Ti_{1.86}$	$Al_{0.49}Ga_{1.65}K_{0.155}O_7Ti_{1.86}$	$Al_{0.84}Ga_{1.30}K_{0.157}O_7Ti_{1.86}$
M_r	347.2	335.4	320.4
Cell setting, space group	Tetragonal, *I*4/*m*	Tetragonal, *I*4/*m*	Tetragonal, *I*4/*m*
a, *c* (Å)	18.0971 (16), 2.9916 (19)	18.0606 (11), 2.9839 (13)	18.0088 (12), 2.9759 (14)
V (Å^3)	979.8 (6)	973.3 (4)	965.1 (5)
Z	8	8	8
D_x (Mg m^{-3})	4.706 (3)	4.576 (2)	4.408 (2)
Radiation type	Mo *Kα*	Mo *Kα*	Mo *Kα*
No. of reflections for cell parameters	20	20	20
θ range (°)	30–37	30–37	30–37
μ (mm^{-1})	13.58	12.21	10.45
Temperature (K)	298	298	298
Crystal form, color	Prism, colorless	Prism, colorless	Prism, colorless
Crystal size (mm)	0.22 × 0.08 × 0.08	0.24 × 0.14 × 0.08	0.20 × 0.03 × 0.02
Data collection			
Diffractometer	Rigaku AFC-5S	Rigaku AFC-5S	Rigaku AFC-5S
Data collection method	$\omega/2\theta$	$\omega/2\theta$	$\omega/2\theta$
Absorption correction	Numerical	Numerical	Numerical
T_{min}	0.292	0.250	0.646
T_{max}	0.467	0.423	0.834
No. of measured, independent and observed reflections	5602, 2817, 2350	5591, 2811, 2378	5056, 2709, 1749
Criterion for observed reflections	$I > 2\sigma(I)$	$I > 2\sigma(I)$	$I > 2\sigma(I)$
R_{int}	0.034	0.038	0.055
θ_{max} (°)	50.1	50.1	50.1
Range of *h*, *k*, *l*	$-38 \Rightarrow h \Rightarrow 39$ $0 \Rightarrow k \Rightarrow 39$ $0 \Rightarrow l \Rightarrow 6$	$-38 \Rightarrow h \Rightarrow 38$ $0 \Rightarrow k \Rightarrow 38$ $0 \Rightarrow l \Rightarrow 6$	$-38 \Rightarrow h \Rightarrow 38$ $0 \Rightarrow k \Rightarrow 38$ $0 \Rightarrow l \Rightarrow 6$
No. and frequency of standard reflections	3 every 100 reflections	3 every 100 reflections	3 every 50 reflections
Intensity decay (%)	< 0.8	< 1.2	< 3.9
Refinement			
Refinement on	F^2	F^2	F^2
$R[F^2 > 2\sigma(F^2)]$, $wR(F^2)$, *S*	0.031, 0.051, 1.10	0.032, 0.055, 1.17	0.043, 0.072, 0.99
No. of reflections	2817	2811	2709
No. of parameters	86	86	86
Weighting scheme	Based on measured s.u.s; $w = 1/[\sigma^2(I) + 0.0001I^2]$	Based on measured s.u.s; $w = 1/[\sigma^2(I) + 0.0001I^2]$	Based on measured s.u.s; $w = 1/[\sigma^2(I) + 0.0001I^2]$
$(\Delta/\sigma)_{max}$	0.001	0.001	0.017
$\Delta\rho_{max}$, $\Delta\rho_{min}$ (e Å^{-3})	1.35, −1.39	2.22, −1.41	2.28, −1.99
Extinction method	B-C type 1 Gaussian isotropic (Becker & Coppens, 1974)	B-C type 1 Gaussian isotropic (Becker & Coppens, 1974)	B-C type 2 (Becker & Coppens, 1974)
Extinction coefficient	0.0397 (6)	0.0609 (9)	0.059 (2)

Computer programs used: *JANA*2000 (Petricek & Dusek, 2000).

$R_{7,2725,0.005} = 1.0038$ for sample (II) and $R_{7,2623,0.005} = 1.0039$ for sample (III). The ratios of reliability factors of harmonic and anharmonic models, $wR_{all,h}(F^2)/wR_{all,anh}(F^2)$ = 5.13/5.06 = 1.014 for sample (I), 5.55/5.48 = 1.013 for sample (II) and 7.21/7.15= 1.008 for sample (III), are larger than the critical value for each sample. Therefore, the above hypothesis can be rejected at the 0.5% significance level for all samples. Thus, the results with anharmonic ADPs were taken as the final ones. The PDF and joint-PDF (Bachmann & Schulz, 1984) for the K ion were obtained from the structural parameters obtained. Absorption corrections were carried out using the program *ACACA* (Wuensch & Prewitt, 1965). The program package *JANA* 2000 (Petricek & Dusek, 2000) was used for the least-squares refinement and other calculations.

3. Results and discussion

3.1. Host framework

The variation in cell dimensions was proportional to *y*, the Al/(Ga + Al) ratio in the crystal. The greater the Al/(Ga + Al) ratio, the smaller the cell dimension. This is reasonable from a crystal chemistry viewpoint because the ionic radius of the Al ion (four-coordinate: 0.39 Å; six-coordinate: 0.535 Å) is smaller than that of four-coordinate Ga with 0.47 Å and six-coordinate Ga with 0.62 Å (Shannon, 1976). The framework structures of $K_x(Ga_{1-y}Al_y)_{2+x}Ti_{2-x}O_7$ ($x \simeq 0.14$, $y \simeq 0.10$, 0.23, 0.39) were basically identical to that of $K_xGa_{2+x}Ti_{2-x}O_7$ ($x \simeq 0.14$) (Watanabe, Sasaki *et al.*, 1987). The occupation factors of the Al and the Ga ions at the metal positions were

plotted against the composition parameter y (Fig. 3). The fraction of the Al ions at each metal position increases with increasing y. It should be noted that the Al/Ga ratio at the individual metal site is remarkably different from site to site; 0.069 ($M1$), 0.102 ($M2$) and 0.339 ($M3$) in sample (I), 0.191 ($M1$), 0.274 ($M2$) and 0.919 ($M3$) in sample (II), 0.405 ($M1$), 0.747 ($M2$) and 1.925 ($M3$) in sample (III). This can be explained from the crystal chemistry viewpoint as follows. As the ionic radius of the oxygen ion is 1.38 Å in four coordination and 1.40 Å in six cooridination (Shannon, 1976), the ideal GaO distances are 1.85 Å in a tetrahedron and 2.02 Å in an octahedron. In $K_xGa_{2+x}Ti_{2-x}O_7$ the mean $M1$—O distance is 1.842 Å (Watanabe, Sasaki *et al.*, 1987), which means that the $M1$ site is almost ideal for the tetrahedrally coordinated Ga ion. On the other hand, the mean distances of $M2$—O (1.990 Å) and $M3$—O (1.962 Å) in $K_xGa_{2+x}Ti_{2-x}O_7$ suggest that these octahedral sites are a little small for the Ga ion. Considering that the Al ion is smaller that the Ga ion, it is natural that the Al/Ga ratios at the octahedral sites, especially at the $M3$ site, are higher than that at the tetrahedral $M1$ site in Al-substituted samples.

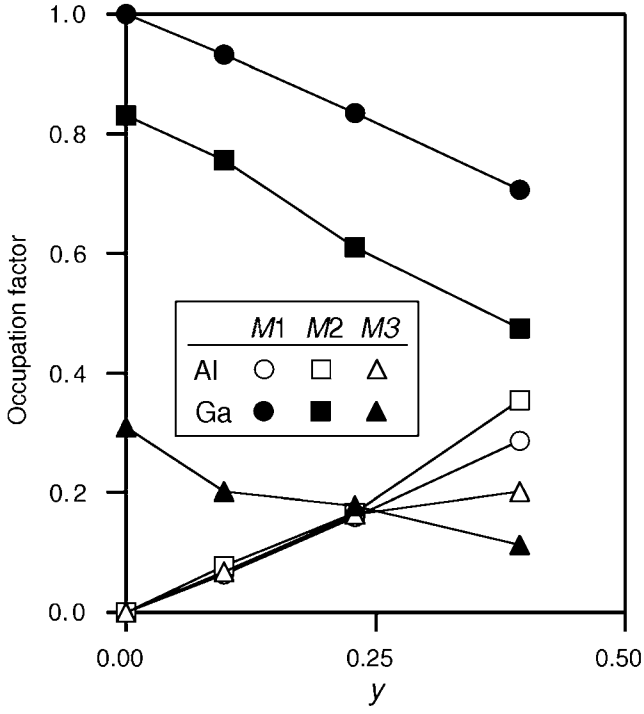

Figure 3
Composition dependence of the occupation factor for the Al and Ga ions at the metal site. y is the parameter for the chemical composition of the crystal $K_x(Ga_{1-y}Al_y)_{2+x}Ti_{2-x}O_7$ ($x \simeq 0.14$).

Table 3
Structural parameters for the K ion.

	Sample (I)	Sample (II)	Sample (III)
Occupancy	0.303 (3)	0.309 (4)	0.314 (5)
z†	0.234 (3)	0.225 (6)	0.226 (3)
U^{11}‡	0.052 (2)	0.051 (2)	0.058 (4)
U^{33}	0.163 (19)	0.18 (3)	0.140 (12)
U_{eq}	0.089 (6)	0.092 (11)	0.085 (5)
C^{113}	−0.0070 (12)	−0.0066 (13)	−0.0080 (19)
C^{333}	1.1 (4)	0.8 (5)	1.9 (4)
D^{1111}	−0.00037 (6)	−0.00027 (5)	−0.00007 (13)
D^{1112}	0.00004 (4)	0.00007 (4)	0.00000 (8)
D^{1122}	−0.00012 (4)	−0.00011 (4)	−0.00018 (8)
D^{1133}	0.009 (4)	0.007 (4)	0.010 (5)
D^{3333}	−9.0 (9)	−7.0 (10)	−10.7 (10)

† The fractional coordinates are $(0, 0, z)$. ‡ $U^{22} = U^{11}$, $U^{12} = U^{13} = U^{23} = 0$. $C^{223} = C^{113}$, $C^{111} = C^{112} = C^{122} = C^{123} = C^{133} = C^{222} = C^{233} = 0$. $D^{1222} = -D^{1112}$, $D^{2222} = D^{1111}$, $D^{2233} = -D^{1133}$, $D^{1113} = D^{1123} = D^{1223} = D^{1233} = D^{1333} = D^{2223} = D^{2333} = 0$. Third-order parameters C^{ijk} are multiplied by 10^3. Parameters D^{ijkl} are multiplied by 10^4.

The mean metal–oxygen distances in the tetrahedron ($M1O_4$) and the octahedra ($M2O_6$, $M3O_6$, $M4O_6$), given in the supplementary material, decrease with increasing y. The tunnel wall is constructed of the alternate stacking of two squares of oxygen ions, the O6 square consisting of four O6 ions and the O7 square consisting of four O7 ions, as seen in Fig. 1. The diagonal distances of the squares in $K_xGa_{2+x}Ti_{2-x}O_7$ and the three samples are 6.156 (11) ($K_xGa_{2+x}Ti_{2-x}O_7$), 6.1343 (16) [sample (I)], 6.1161 (15) [sample (II)] and 6.100 (3) Å [sample (III)] for O6—O6, and 6.517 (11) ($K_xGa_{2+x}Ti_{2-x}O_7$), 6.4844 (18) [sample (I)], 6.4764 (17) [sample (II)] and 6.470 (3) Å [sample (III)] for O7—O7. It is natural that the contraction of coordination polyhedra due to the substitution of the Al ion for Ga, accompanying the decrease in cell dimensions, gives rise to the contraction of the tunnel section. Thus, the structural data obtained for the host frame-

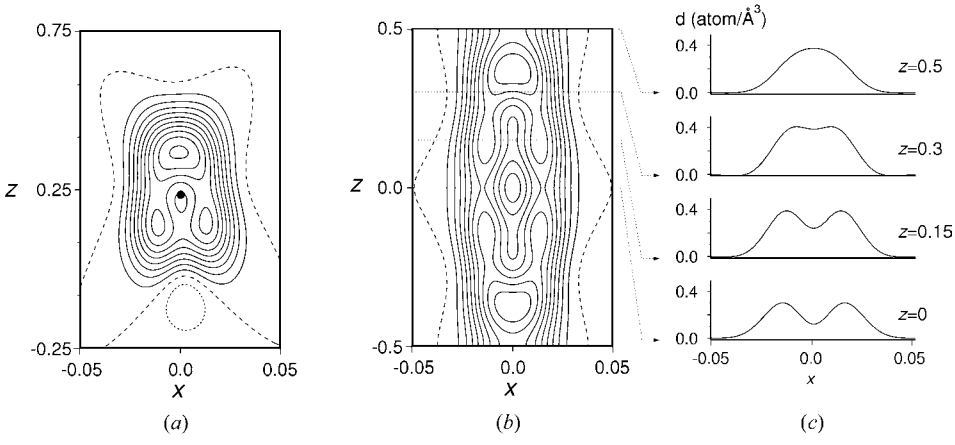

Figure 4
(*a*) PDF, (*b*) joint-PDF of the K ion at the section $y = 0$, and (*c*) joint-PDF on $(y, z) = (0, 0)$, $(0, 0.15)$, $(0, 0.3)$, $(0, 0.5)$ for sample (I). Contour intervals are 0.05 atom Å^{-3}. Broken lines in (*a*) and (*b*) indicate the zero level. The filled circle in (*a*) is the basic position of the K ion.

work, such as occupation ratios and interatomic distances, are generally consistent with each other from a crystal chemistry viewpoint.

3.2. Probability density of the K ion

Structural parameters relating to the K ion are listed in Table 3. In ideal compositions of $K_x(Ga_{1-y}Al_y)_{2+x}Ti_{2-x}O_7$ ($x \simeq 0.14$, $y \simeq 0.10$, 0.23 and 0.39), the occupation factor of the K ion at the 4(*e*) site (0, 0, *z*) should be *ca* 0.28. However, an excessive number of K ions were observed in refinements for all the samples as well as in $K_xGa_{2+x}Ti_{2-x}O_7$ ($x \simeq 0.14$; Watanabe *et al.*, 1992). This was attributed to the introduction of excessive K_2O in the tunnel, which was consistent with the results from EPMA. Thus, the composition was strictly given as $K_x(Ga_{1-y}Al_y)_{2+x}Ti_{2-x}O_7 + zK_2O$ or $K_{x+2z}(Ga_{1-y}Al_y)_{2+x}Ti_{2-x}O_{7+z}$, where *z* was estimated to be 0.0115 for sample (I), 0.0145 for sample (II) and 0.017 for sample (III). Additional oxygen ions seem to be distributed in the tunnels, but these were ignored in the refinements because of the difficulty in discriminating them from K ions. Electrons due to the excessive oxygen ions were 3–4% of those from the K ions. As seen in Fig. 1, the tunnel with the (0, 0, *z*) central axis is equivalent to the tunnel with the ($\frac{1}{2}$, $\frac{1}{2}$, *z*) center axis, because the structure has the body-centered lattice. In order to avoid confusion, the first tunnel with the (0, 0, *z*) center axis is used for discussion hereafter. The same discussion is applicable to the second tunnel, although the fractional coordinate for *z* is to be shifted by $\frac{1}{2}$ due to the ($\frac{1}{2}$, $\frac{1}{2}$, $\frac{1}{2}$) centering translation. The probability density functions (PDFs) for the K ion and the joint-PDFs including equivalent K ions were calculated from the final parameters. The maps at the $y = 0$ section of sample (I) are shown in Fig. 4, where the distribution of the K ion is almost continuous along the tunnel. The other two samples exhibited similar features in their K-ion distributions. It should be noted that the local density at (0, 0, 0) is not the maximum, but the minimum. This means that the K conduction path, which is defined as the path connecting the positions of the highest density at each *z* level, deviates from the center axis of the tunnel in the range $|z| \leq ca$ 0.3, as seen in Fig. 4(*c*). The joint-PDF maps at the $z = 0$ section for the three samples (Figs. 5*a*, *c* and *e*) clearly show four peaks at positions away from the origin. These results indicate that the tunnel section around $z = 0$, which is defined by the O7 square, is so large that the K ion is more stabilized by following the paths which deviate from the center axis of the tunnel rather than remaining on

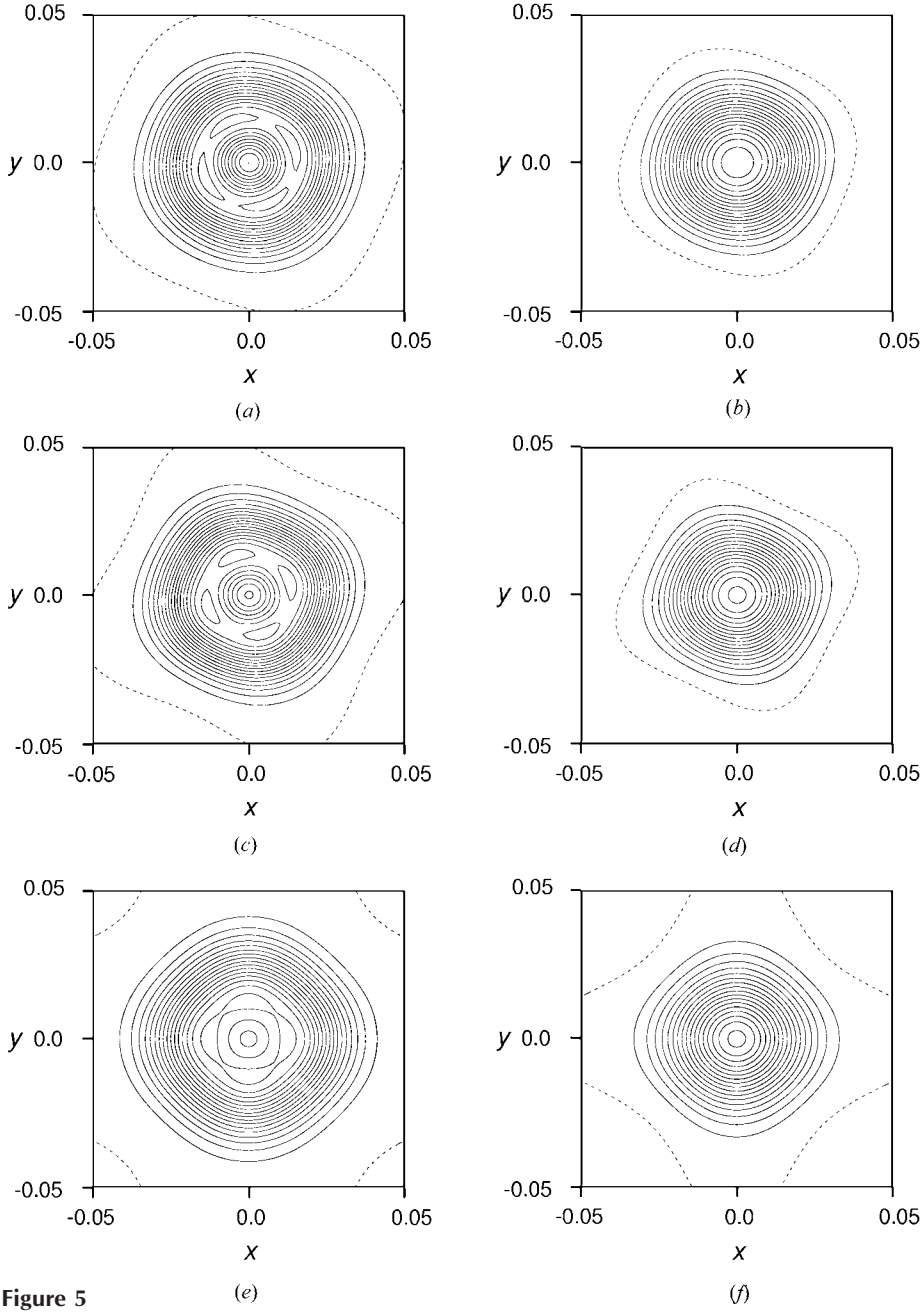

Figure 5
Joint-PDF of the K ions for (*a*) sample (I) at the $z = 0$ section, (*b*) sample (I) at $z = 1/2$, (*c*) sample (II) at $z = 0$, (*d*) sample (II) at $z = 1/2$, (*e*) sample (III) at $z = 0$ and (*f*) sample (III) at $z = 1/2$. Contour intervals are 0.02 atom Å^{-3}. Broken lines indicate the zero level. Note that the origin (0 0 0) is locally not the maximum, but the minimum in maps (*a*), (*c*) and (*e*). Maximum densities in these maps are observed at the four equivalent positions displaced close to the origin. In (*b*), (*d*) and (*f*), the center position (x, y) = (0, 0) has the maximum density.

the center axis (0, 0, z). In the joint-PDFs at the $z = 0$ section for the three samples, the peak maxima are at (x, y) = (0.005, −0.014) in sample (I), (0.005, −0.013) in sample (II) and (0.000, 0.013) in sample (III) and their equivalent positions. The distance from the origin to the peaks becomes shorter according to the increase in the Al content of the structure; 0.273 Å for sample (I), 0.253 Å for sample (II), and 0.234 Å for sample (III). Namely, the deviation of the conduction path from the center axis of the tunnel decreases according to the increase in the Al content. This is consistent with the variation in the diagonal O7—O7 distance of the O7 square mentioned in §3.1. The deviation of the conduction path must be more prominent in $K_xGa_{2+x}Ti_{2-x}O_7$ than in sample (I), because the diagonal O7—O7 distance is longer in the former than in the latter. However, it is impossible to discuss the deviation of the path in $K_xGa_{2+x}Ti_{2-x}O_7$, because the structure refinement of $K_xGa_{2+x}Ti_{2-x}O_7$ with anharmonic ADPs has never been carried out. On the other hand, the joint-PDFs at $z = \frac{1}{2}$ showed a peak at the center of the (0, 0, $\frac{1}{2}$) tunnel section in all the samples (Figs. 5*b*, *d* and *f*). This is because the diagonal O6—O6 distance of the O6 square at $z = \frac{1}{2}$ is smaller than that of the O7 square at $z = 0$. However, the effective diameters of the O6 squares, given by the diagonal distance subtracted by twice the ionic radius of the O ion (1.40 Å), which are 3.334 for sample (I), 3.316 for sample (II) and 3.300 Å for sample (III), are still larger than the diameter of the 12-coordinate K ion, 3.28 Å (Shannon, 1976). Therefore, it is speculated that the oxygen squares in $K_x(Ga_{1-y}Al_y)_{2+x}Ti_{2-x}O_7$ do not play the *bottleneck* role, which is supported by the joint-PDF maps.

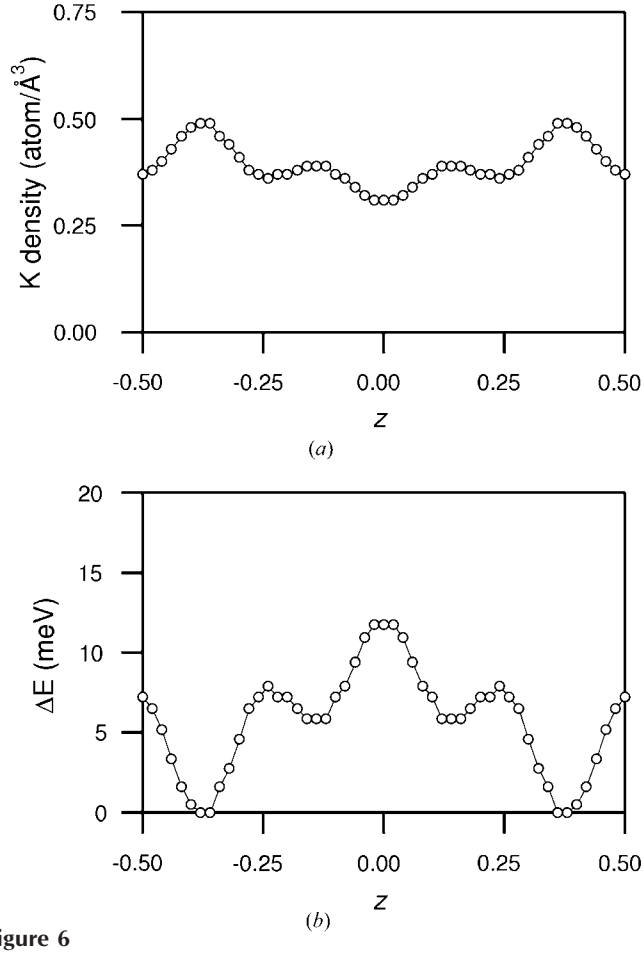

Figure 6
(*a*) Joint-PDF and (*b*) the one-particle potential for the K ion along the conduction path in $K_x(Ga_{1-y}Al_y)_{2+x}Ti_{2-x}O_7$ ($x \simeq 0.14$, $y \simeq 0.10$).

The one-particle potentials (OPPs) for the K ion were calculated from the joint-PDFs along the conduction path, as shown for sample (I) (Fig. 6). The maximum potential value in the curves was 12 meV for sample (I), 11 meV for sample (II) and 17 meV for sample (III). These values are far smaller than the barrier heights obtained from other one-dimensional ionic conductors at room temperature: 32 meV for hollandite $K_{1.54}Mg_{0.77}Ti_{7.23}O_{16}$ (Weber & Schulz, 1986) and 39 meV for $Na_{0.8}Ti_{1.2}Ga_{4.8}O_{10}$ (Michiue & Sato, 2004). The barrier height from the X-ray diffraction study for hollandite is roughly in agreement with the activation energies obtained from the conductivity measurement of 34 (Khanna *et al.*, 1981) and 58 meV (Yoshikado *et al.*, 1982) at microwave frequencies. On the other hand, there are significant discrepancies seen between the energy barriers from the X-ray diffraction and the AC impedance measurement for $K_x(Ga_{1-y}Al_y)_{2+x}Ti_{2-x}O_7$ ($x \simeq 0.14$, $y \simeq 0.10, 0.23, 0.39$). Activation energies of *ca* 40–70 meV were obtained from the temperature dependence of the complex conductivity for $K_x(Ga_{1-y}Al_y)_{2+x}Ti_{2-x}O_7$ ($x \simeq 0.14$, $y \simeq 0.10, 0.23, 0.39$; Yoshikado *et al.*, 1992). These facts are explained by the structural aspect of the materials, that is whether the conduction ion suffers the *bottleneck effect* or not. In the hollandite structure, the tunnel wall is constructed of the alternate stacking of the two squares of oxygen ions with considerably different sizes; the smaller square at $z = 0$ and the larger one at $z = \frac{1}{2}$. The diagonal distance of the smaller square is *ca* 5.2 Å (5.22 Å in $K_{1.54}Mg_{0.77}Ti_{7.23}O_{16}$ and 5.18 Å in $K_{1.50}Al_{1.50}Ti_{6.50}O_{16}$; Watanabe, Fujiki *et al.*, 1987). The effective diameter of the square is 2.4 Å, which is 0.34 Å smaller than the diameter of the four-coordinate K ion, 2.74 Å. Another square at $z = \frac{1}{2}$ is large enough to allow the K ion to remain at its center. Therefore, (0, 0, $\frac{1}{2}$) is suitable for the location of the K ion forming a so-called cuboctahedral coordination with 12 oxygen ions: eight oxygen ions of the two smaller squares at $z = 0$ and $z = 1$, and four additional oxygen ions of the larger square at $z = \frac{1}{2}$. Thus, the tunnel in the hollandite structure is regarded as a linear connection of the cavities. The cavities are partially occupied (*ca* 77% in $K_{1.54}Mg_{0.77}Ti_{7.23}O_{16}$) by K ions. The K ion in a cavity can move to a neighbouring cavity, if it is vacant. In this process the boundary of the two cavities, which is the smaller oxygen-ion square, acts as a *bottleneck*. Namely, in the usual ionic conductors with mobile ions suffering the *bottleneck effect*, the ionic conduction process is approximated by the hopping of each mobile ion between the stable sites (*i.e.* the potential minima), although the interaction between mobile ions must be carefully considered. On the other hand, the ionic conduction in $K_x(Ga_{1-y}Al_y)_{2+x}Ti_{2-x}O_7$ with no *bottleneck effect* is better explained by a model in which the collective motion of the K ions forming clusters is dominant (Yoshikado *et al.*, 1992) rather than the local hopping of individual K ions. This might be the reason why energy barriers from X-ray

diffraction are significantly lower than those from the AC impedance measurement in the case of $K_x(Ga_{1-y}Al_y)_{2+x}Ti_{2-x}O_7$.

In conclusion, the following has been clarified by the present study.

(i) The host framework of the $K_xGa_{2+x}Ti_{2-x}O_7$ structure is basically retained during Al substitution for at least *ca* 40% of Ga ions.

(ii) The composition dependences of the interatomic distances in $K_x(Ga_{1-y}Al_y)_{2+x}Ti_{2-x}O_7$ ($x \simeq 0.14$, $y \simeq 0.10$, 0.23, 0.39) were reasonably explained from the crystal chemistry viewpoint.

(iii) The conduction path of the K ion partially deviates from the center axis of the tunnel in $K_x(Ga_{1-y}Al_y)_{2+x}Ti_{2-x}O_7$.

(iv) No distinct *bottleneck effect* was observed from joint-PDFs and OPPs for the K ion in $K_x(Ga_{1-y}Al_y)_{2+x}Ti_{2-x}O_7$, which strongly supports the assumption that the conduction mechanism in $K_xGa_{2+x}Ti_{2-x}O_7$-type compounds is different from that in the more typical one-dimensional ionic conductors such as hollandite.

One of the authors (YM) is grateful to Mr Kosuke Kosuda in NIMS for the measurement of EPMA.

References

Bachmann, R. & Schulz, H. (1984). *Acta Cryst.* A**40**, 668–675.
Becker, P. J. & Coppens, P. (1974). *Acta Cryst.* A**30**, 129–147.
Hamilton, W. C. (1965). *Acta Cryst.* **18**, 502–510.
Johnson, C. K. & Levy, H. A. (1974). *International Tables for X-ray Crystallography*, Vol. IV, pp. 311–336. Birmingham: Kynoch Press.
Khanna, S. K., Gruner, G., Orbach, R. & Beyeler, H. U. (1981). *Phys. Rev. Lett.* **47**, 255–257.
Kuhs, W. F. (1992). *Acta Cryst.* A**48**, 80–98.
Michiue, Y. & Sato, A. (2004). *Acta Cryst.* B**60**, 692–697.
Onoda, Y., Watanabe, M., Fujiki, Y., Yoshikado, S., Ohachi, T. & Taniguchi, I. (1989). *Solid State Ion.* **35**, 387–394.
Onoda, Y., Watanabe, M., Fujiki, Y., Yoshikado, S., Ohachi, T. & Taniguchi, I. (1990). *Solid State Ion.* **40/41**, 147–149.
Petricek, V. & Dusek, M. (2000). *JANA*2000. Institute de Physics, Praha, Czech Republic.
Shannon, R. D. (1976). *Acta Cryst.* A**32**, 751–767.
Watanabe, M., Fujiki, Y., Kanazawa, Y. & Tsukimura, K. (1987). *J. Solid State Chem.* **66**, 56–63.
Watanabe, M., Fujiki, Y., Kosuda, K., Yoshikado, S. & Ohachi, T. (1992). *Solid State Ion.* **53–56**, 784–790.
Watanabe, M., Fujiki, Y., Yoshikado, S. & Ohachi, T. (1988). *Solid State Ion.* **28–30**, 257–261.
Watanabe, M., Fujiki, Y., Yoshikado, S., Ohachi, T. & Kudo, Y. (1990). *Solid State Ion.* **40/41**, 139–141.
Watanabe, M., Sasaki, T., Kitami, Y. & Fujiki, Y. (1987). *Acta Cryst.* C**43**, 392–395.
Weber, H.-P. & Schulz, H. (1986). *J. Chem. Phys.* **85**, 475–484.
Wuensch, A. D. & Prewitt, C. T. (1965). *Z. Kristallogr.* **1**, 24–59.
Yoshikado, S., Funatomi, H., Taniguchi, I., Watanabe, M., Onoda, Y. & Fujiki, Y. (1996). *Solid State Ion.* **86–88**, 1325–1329.
Yoshikado, S., Funatomi, H., Watanabe, M., Onoda, Y. & Fujiki, Y. (1999). *Solid State Ion.* **121**, 127–132.
Yoshikado, S., Ohachi, T., Taniguchi, I., Onoda, Y., Watanabe, M. & Fujiki, Y. (1982). *Solid State Ion.* **7**, 335–344.
Yoshikado, S., Ohachi, T., Taniguchi, I., Watanabe, M., Fujiki, Y. & Onoda, Y. (1988). *Solid State Ion.* **28–30**, 173–178.
Yoshikado, S., Ohachi, T., Taniguchi, I., Watanabe, M., Onoda, Y. & Fujiki, Y. (1990). *Solid State Ion.* **40/41**, 142–146.
Yoshikado, S., Ohachi, T., Taniguchi, I., Watanabe, M., Onoda, Y. & Fujiki, Y. (1992). *Solid State Ion.* **53–56**, 754–762.